Forced traveling waves in a reaction-diffusion equation with strong
Allee effect and shifting habitat

Bingtuan Li* Garrett Otto †

- ⁴ Key words. Reaction-diffusion equation, Allee effect, shifting habitat, traveling wave
- 6 AMS subject classification. 92D40, 92D25

3

8 Abbreviated title. Traveling waves in a reaction-diffusion equation

 $^{^*}$ Department of Mathematics, University of Louisville, Louisville, KY 40292. B. Li was partially supported by the National Science Foundation under Grant DMS-1951482

 $^{^\}dagger \mbox{Department}$ of Mathematics, SUNY Cortland, Cortland, NY 13045

9 Abstract

We study a reaction-diffusion equation that describes the growth of a population with a strong Allee effect in a bounded habitat which shifts at a speed c>0. We demonstrate that the existence of forced positive traveling waves depends on habitat size L, and c^* , the speed of traveling wave for the corresponding reaction-diffusion equation with the same growth function all over the entire unbounded spatial domain. It is shown that for $c^*>c>0$ there exists a positive number $L^*(c)$ such that for $L>L^*(c)$ there are two positive traveling waves and for $L<L^*(c)$ there is no positive traveling wave. It is also shown if $c>c^*$ for any c>c0 there is no positive traveling wave. The dynamics of the equation are further explored through numerical simulations.

18 1 Introduction

Climate change has resulted in poleward and upslope range shifts in many species across the globe, and it becomes important whether or not species maintain in their current ranges (Parmesan and Yohe [36], Parmesan [37], Walther et al. [43]). Species may respond to climate change by shifting their distribution or phenology, acclimating or adapting to changes; however the inability to sufficiently adapt will result in extinction (Aitken et al. [1], Cleland et al. [11], Valladares et al. [42]). Species potential to successfully adapt or shift distributions in response to climate change depends on a host of factors, such as the speed and variability of changing conditions, species' dispersal abilities, characteristics of a species climatic niche and species interactions. Several reaction-diffusion models have been developed to explore species persistence using shifting boundary conditions or shifting growth functions (Berestycki et al. [7], Li et al. [24], MacDonald and Lutscher [31], Potapov and Lewis [39]).

The early work by Potapov and Lewis [39] conceptualized the shifting suitable habitat of a species. The single-species version of their model takes the form

$$u_t = u_{xx} + f(u, x - ct),$$
 (1.1)

 $_{\scriptscriptstyle 1}$ with

$$f(u,z) = \begin{cases} g(u) & \text{if } 0 \le z \le L, \\ -ru, & \text{if } z < 0 \text{ or } z > L. \end{cases}$$
 (1.2)

Here u(x,t) is the density of a population at location x and time t, f(u,x-ct) describes the population growth at point x at time t, c is the speed at which the habitat shifts, L and r are positive constants, and g satisfies g(0) = g(1) = 0 and g(u) > 0 on (0,1). g(u) exhibits monostability, and a prototype example is g(u) = u(1-u). In this model the population grows in the interval [0,L] and declines outside this interval. Berestycki et al. [7] provided the critical length of L and showed that for L above the critical length equation (1.1) has a globally attracting nontrivial forced traveling wave with speed c. The authors extended the results to a general class of equations by studying the eigenvalue problem of a linearized system. MacDonald and Lutscher [31] extended the results in [7] by including individual movement behavior at habitat edges. Piecewise growth functions similar to (1.2) have been also used to study promotion zones and barrier zones for species persistence and spread in heterogeneous environments (Du et al. [15] and Li et al. [27]).

The equation (1.1) has also been investigated for f(u,x) in other forms different from (1.2). Li et al. [24] and Hu et al. [13] considered spreading speeds for (1.1) where f(u,x-ct) = u(s(x-ct)-u) and s(x) is a nondecreasing function for $-\infty < x < \infty$. Bouhours and Giletti [9] studied the spreading and vanishing dynamics for a general two-dimensional reaction-diffusion equation which includes f(u,x-ct)

of traveling waves for a one-dimensional reaction-diffusion equation with a general nonlinear growth function f(x-ct,u). The results in [8] allow both $s(\infty)$ and $s(-\infty)$ to have same sign in the case of f(x-ct,u) = u(s(x-ct)-u). For more results regarding traveling waves for reaction-diffusion equations with a shifting habitat, the reader is referred to Berestycki et al. [7], Berestycki and Rossi [5, 6], Hamel [19], Hamel and Roques [20], and Fang et al. [16]. Mathematical models have been developed in other forms that are used to describe species development in shifting habitats; see, for example, Zhou and Kot [45], Li et al. [25, 27], and Li et al. [29], where integro-difference equations and integro-differential equations are involved.

The aforementioned papers assume no Allee effect in species growth. An Allee effect arises when the per-capita birth rate increases at lower population densities, and a strong Allee effect is an Allee effect with a critical population density [2, 35]. There are cases where Allee effects occur when species distributions shift in response to climate change (Livshultz et al. [30], Samuel and Chandler [40], Shanks et al. [41], Wood et al. [44]). It is of great interest to explore the population dynamics of species with a strong Allee effect in a shifting habitat. In this paper we study (1.1) and (1.2) where g has a strong Allee effect, i.e., bistability. The reaction-diffusion equation

$$u_t = u_{xx} + g(u), \quad -\infty < x < \infty, \tag{1.3}$$

with g(u) exhibiting bistability has been well studied (see Fife [17] and references cited therein). It is well-known that there exists a real number c^* which is the unique speed of traveling waves connecting zero to the carrying capacity, and the sign of c^* is the same as that of the integral of g(u) from zero to the carrying capacity. c^* can be calculated using variation techniques (Benguria and Depassier [4]) when it is positive.

In this paper, we study whether or not a species governed by (1.1) with (1.2) and a strong Allee effect can keep pace with a shifting habitat. We find that the wave speed c^* and the habit shift speed c both play important roles in determining species persistence. We particularly establish the existence forced positive traveling waves. A positive traveling wave is a nonnegative traveling wave which is not uniformly zero valued. We show that if $c^* > c > 0$ there exists a positive number $L^*(c)$ such that for $L > L^*(c)$ there are two positive traveling waves and for $L < L^*(c)$ there is no positive traveling wave, and if $c > c^*$ for any L > 0 there is no positive traveling wave. We provide numerical simulations to further examine the behavior of the system. Our numerical results demonstrate that the larger traveling wave attracts solutions with proper initial data so that persistence takes place, and in case of no traveling wave, solutions approach zero and extinction occurs.

This paper is organized as follows. The analytical results regarding the existence of traveling waves are presented in Section 2. The numerical simulations are given in Section 3. Some concluding remarks are provided in Section 4.

2 Main results

We begin with the following hypotheses to address the presence of a strong Allee effect in q:

83 Hypotheses 2.1.

```
i. g(u) \in C^1[0,1], g(0) = g(1) = 0, g'(0) < 0, g'(1) < 0, and there is a number a such that 0 < a < 1, g(a) = 0, g(u) < 0 on (0,a), and g(u) > 0 on (a,1).
```

ii. g'(0) > -r.

Hypotheses 2.1 (i) indicates that g(u) exhibits a strong Allee effect with a the Allee threshold and 1 the (scaled) carrying capacity. A protype example is g(u) = u(u - a)(1 - u) with 0 < a < 1. Hypotheses 2.1 (ii) assumes that the population decay rate at low densities in the moving patch is less than that outside the patch. Biologically this means the environment outside the growth zone is harsher than that inside the patch. We shall consider c > 0 as the case of c < 0 can be treated in a similar way.

The function f(u,x) is discontinuous at x=0,L. Following Berestycki et al. [7], we seek traveling wave solutions for (1.1), which are globally of class C^1 (indeed, to guarantee that diffusion conserves mass, the flux u_x should be continuous [7]) and piecewise of class C^2 and satisfy the equation at each point with $x \neq 0, L$. It is known that the problem of (1.1) with appropriate initial data u(x,0) has a unique, globally defined, solution u=u(x,t), which, as a function of x has such smoothness (Berestycki et al. [7] and Du et al. [15]). Berestycki et al. [7] determined the critical patch size and established the existence of a positive traveling wave for $g(u) = \tilde{r}u(1-\frac{u}{\tilde{k}})$ with $\tilde{r} > 0$ and $\tilde{k} > 0$ by glueing phase portraits. There is long history of using phase portrait analysis to study traveling waves; see for example Fife [17] and references cited therein. For some recent work on phase portrait analysis for systems with a strong Allee effect and stationary habitat, the reader may refer to Pouchol et al. [38] and Li et al. [27, 28].

We have the following proposition (see Fife [17]).

Proposition 2.1. Assume that Hypotheses 2.1 (i) is satisfied. Then the equation (1.3) has a unique nonincreasing traveling wave solution (up to translation) $u(x,t) = w^*(x-c^*t)$ with $w^*(-\infty) = 1$ and $w^*(\infty) = 0$. Furthermore, $c^* > 0$ if and only if $\int_0^1 g(u)du > 0$, $c^* = 0$ if and only if $\int_0^1 g(u)du = 0$, and $c^* < 0$ if and only if $\int_0^1 g(u)du < 0$.

For g(u) = u(u-a)(1-u), the unique traveling wave speed is $c^* = \frac{1-2a}{\sqrt{2}}$ (see Hadeler and Rothe [18] and Nagumo et al. [34]). In general for $\int_0^1 g(u)du > 0$ (i.e., $c^* > 0$), c^* can be obtained using the following variational formula given by Benguria and Depassier [4]:

$$(c^*)^2 = \max_{h(u) \in C^1[0,1], h'(u) < 0} \left\{ \frac{2 \int_0^1 g(u)h(u)du}{\int_0^1 (-h^2(u)/h'(u))du} \right\}.$$

A traveling wave u(x,t) = w(x-ct) for (1.3) satisfies

$$w''(z) + cw'(z) + g(w(z)) = 0, (2.1)$$

with z = x - ct. This is equivalent to the planar system

$$w' = v,$$

$$v' = -cv - g(w).$$
(2.2)

Phase plane analysis for the existence of a traveling wave for (2.2) can be found in [17]. We further analyze (2.2) in order to study traveling waves for (1.1) with (1.2). System (2.2) has three equilibria

113 (0,0), (a,0) and (1,0). For $c \ge 0$, both (0,0) and (1,0) are saddles. For convenience, we use S_0^c and U_0^c to denote the stable and unstable manifolds of (0,0) corresponding to c for 0 < w < 1, respectively, and 115 use S_1^c and U_1^c to denote the stable and unstable manifolds of (1,0) corresponding to c for 0 < w < 1, 116 respectively.

The Jacobian matrix of (2.2) is

$$J = \left(\begin{array}{cc} 0 & 1 \\ -g'(w) & -c \end{array} \right).$$

117 At (0,0) the eigenvalues are $\lambda_0^{\pm} = \frac{-c \pm \sqrt{c^2 - 4g'(0)}}{2}$. The corresponding eigenvectors are given by $\begin{pmatrix} 1 \\ \lambda_0^{\pm} \end{pmatrix}$.

At (1,0) the eigenvalues are $\lambda_1^+ = \frac{-c \pm \sqrt{c^2 - 4g'(1)}}{2}$, and the corresponding eigenvectors are given by $\begin{pmatrix} 1 \\ \lambda_1^{\pm} \end{pmatrix}$. Clearly, $\lambda_0^+ > 0$, $\lambda_1^+ > 0$, $\lambda_0^- < 0$, and $\lambda_1^- < 0$. All the eigenvalues λ_0^{\pm} and λ_1^{\pm} decrease in c.

Note that here a stable or unstable manifold of an equilibrium is tangent to the line passing through the equilibrium with the slope determined by the corresponding eigenvector. These lead to the following lemma.

Lemma 2.1. Assume that Hypotheses 2.1 hold and $c \ge 0$. We have the following statements for (2.2):

- i. Near (0,0), S_0^c lies below the w-axis and U_0^c lies above the w-axis. Furthermore for $c_2 > c_1 \ge 0$, near (0,0), $S_0^{c_2}$ is below $S_0^{c_1}$ and $U_0^{c_2}$ is below $U_0^{c_1}$.
- ii. Near (1,0), S_1^c lies above the w-axis and U_1^c lies below the w-axis. Furthermore for $c_2 > c_1 \ge 0$, near (1,0), $S_1^{c_2}$ is above $S_1^{c_1}$ and $U_1^{c_2}$ is above $U_0^{c_1}$.

Lemma 2.2. Assume that Hypotheses 2.1 hold. We have the following statements for (2.2):

- i. If $c_2 > c_1 \ge 0$, $S_0^{c_2}$ is below $S_0^{c_1}$ whenever v < 0, and $U_0^{c_2}$ is below $U_0^{c_1}$ whenever v > 0.
- ii. If $c_2 > c_1 \ge 0$, $S_1^{c_2}$ is above $S_1^{c_1}$ whenever v > 0, and $U_1^{c_2}$ is above $U_1^{c_1}$ whenever v < 0.

Proof. The proof of the statement (i) is similar to that of Lemma 4.14 in Fife [17] (also see Kanel' [21]). For the sake of completeness, we provide the proof here. When $v \neq 0$, v can be viewed as a function of

w, and

$$\frac{dv}{dw} = -c - \frac{g(w)}{v}. (2.3)$$

Let $v = v_1(w)$ represent $S_0^{c_1}$ and $v = v_2(w)$ represent $S_0^{c_2}$ for v < 0. In view of Lemma 2.1 (i), we choose w_0 to be a small positive number such that $v_1(w) > v_2(w)$ for $0 < w \le w_0$. From (2.3),

$$\frac{dv_1(w)}{dw} - \frac{dv_2(w)}{dw} - \frac{g(w)}{v_1v_2}(v_1 - v_2) = -(c_1 - c_2),$$

so that for

$$D(w) = (v_1(w) - v_2(w))e^{\int_{w_0}^w (-g(y)/(v_1(y)v_2(y)))dy}$$

134 we have

$$\frac{dD(w)}{dw} = (c_2 - c_1)e^{\int_{w_0}^w (-g(y)/(v_1(y)v_2(y)))dw}.$$
(2.4)

Since $\frac{dD(w)}{dw} > 0$ and $v_1(w_0) - v_2(w_0) > 0$, the function D(w) increases for $w > w_0$ and thus is positive whenever $w > w_0$, $v_1 < 0$ and $v_2 < 0$. It follows that $v_1(w) > v_2(w)$ whenever $w > w_0$, 135 136 $v_1(w) < 0$ and $v_2(w) < 0$. This proves the first part of statement (i). The proof of the second part of statement (i) is similar and omitted. 138

We next let $v = v_1(w)$ represent $S_1^{c_1}$ and $v = v_2(w)$ represent $S_1^{c_2}$ for v > 0. In view of Lemma 2.1 (ii), we choose w_0 to be a positive number close to but less than 1 so that $v_1(w) < v_2(w)$ for $w_0 \le w < 1$. (2.4) still holds with these v_1 and v_2 . Since D(w) increases for $w < w_0, v_1(w) < v_2(w)$ whenever $w_0 > w \ge 0$, $v_1(w) > 0$, and $v_2(w) > 0$. This proves the first part of statement (ii). The proof of the second part of statement (ii) is similar and omitted.

Lemma 2.3. Assume that Hypotheses 2.1 hold. Let $c_2 > c_1 \ge 0$. Let $v = v_1(w)$ and $v = v_2(w)$ be the two solutions of (2.3) corresponding to c_i , respectively. Let w_0 be a number such that $1 > w_0 > 0$. 145

- i. If $v_1(w_0) > v_2(w_0) > 0$ then $v_1(w) > v_2(w)$ whenever $1 > w > w_0$, $v_1(w) > 0$ and $v_2(w) > 0$. 146
- ii. If $0 > v_1(w_0) \ge v_2(w_0)$ then $v_1(w) > v_2(w)$ whenever $1 > w > w_0$, $v_1(w) < 0$ and $v_2(w) < 0$. 147
- The proof of this lemma is similar to that of Lemma 2.2 and is omitted. 148
 - When c = 0, the system (2.2) becomes

$$w' = v,$$

$$v' = -g(w),$$
(2.5)

so that for $v \neq 0$,

137

139

141

142

149

$$\frac{dv}{dw} = -\frac{g(w)}{v}$$
.

This system is integrable, and

$$\frac{1}{2}v^2 = -\int g(w)dw.$$

Assume $\int_0^1 g(u)du > 0$. S_0^0 coincides with U_0^0 between 0 < w < 1 forming a homoclinic orbit given by

$$S_0^0$$
 and U_0^0 : $\frac{1}{2}v^2 = -\int_0^w g(s)ds$.

 S_1^0 and U_1^0 between 0 < w < 1 are given by

$$S_1^0: v = \sqrt{2 \int_w^1 g(s) ds}; \quad U_1^0: v = -\sqrt{2 \int_w^1 g(s) ds}.$$

See Fig. 1 (a) for a graphical description of S_0^0 , U_0^0 , S_1^0 , and U_1^0 . In this figure B is the unique number satisfying $\int_0^B g(s)ds = 0$ and a < B < 1.

When $c = c^*$, there is a traveling wave connecting 0 and 1. The corresponding heteroclinic orbit T^* 152 is depicted in Figure 1 (b) 153

For c>0, (2.2) is not integrable. In the w-v plane, the isocline for $\frac{dw}{dz}=0$ is v=0, and the 154 isocline for $\frac{dv}{dz} = 0$ is $v = -\frac{g(w)}{c}$. See Fig. 2 for a graphical demonstration of the direction field.

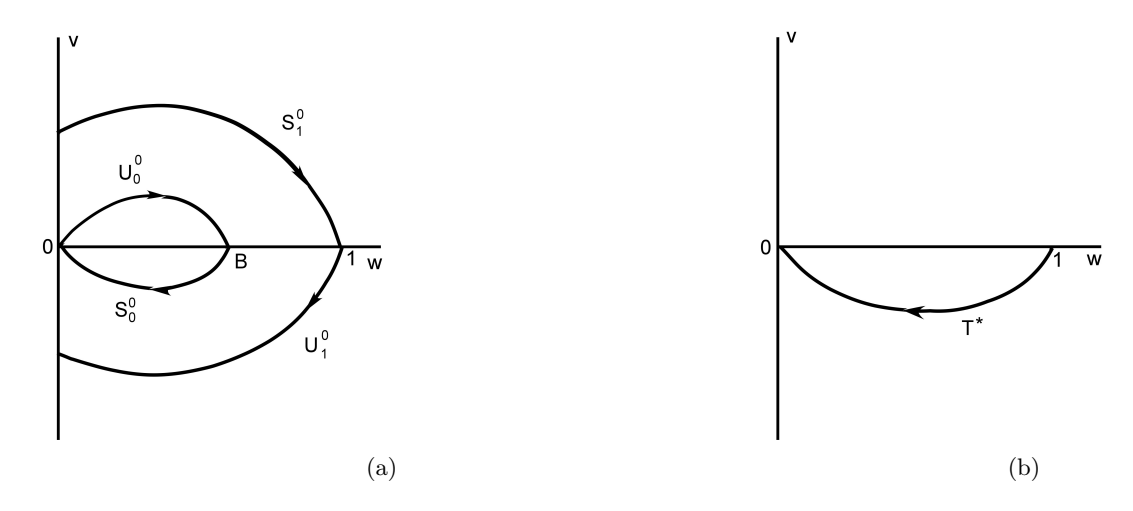


Figure 1: (a) Stable and unstable manifolds of (0,0) and (1,0) for 0 < w < 1 when c = 0. (b) Heteroclinic orbit connecting (0,0) and (1,0) when $c = c^*$.

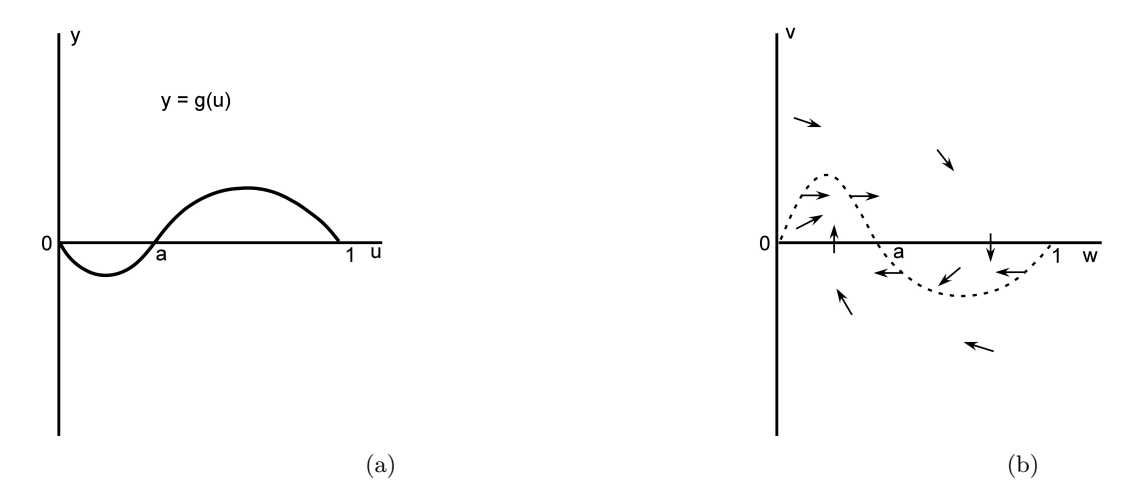


Figure 2: (a) The graph of y=g(u). (b) Direction field: the isocline for $\frac{dw}{dz}=0$ is v=0, and the isocline for $\frac{dv}{dz}=0$ is $v=-\frac{g(w)}{c}$ (dashed curve).

Lemma 2.4. Assume that Hypotheses 2.1 hold and $c^* > c > 0$. We have the following statements:

- i. S_1^c lies above S_1^0 , and below a line v = -m(w-1) for some m > 0.
- ii. U_1^c lies above U_1^0 and below T^* , and U_1^c and S_0^c do not intersect.
- iii. S_0^c lies outside the loop S_0^0 and U_0^0 , below S_1^c , and above U_1^c .
 - iv. U_0^c lies inside the loop S_0^0 and U_0^0 and approaches (a,0).

160

Proof. The first part of statement (i) follows from Lemma 2.2 (ii). S_1^c is tangent to the line passing through (1,0) with the slope $\lambda_0^- = -\frac{\sqrt{c^2 - 4g'(1)} + c}{2} < 0$. For a small $\delta > 0$, there exists a point (w_1, v_1) on S_1^c such that for $w_1 < w < 1$, S_1^c is below the line passing through (1,0) with the slope $\lambda_0^- - \delta$.

Let (w_1, \tilde{v}_1) be the point on S_1^0 . Since S_1^c lies above S_1^0 , we may choose w_1 sufficiently close to 1 such that S_1^c is above the line $v = \tilde{v}_1$ whenever $w_1 > w > 0$. Consequently along S_1^c , $\frac{g(w)}{v} \leq \frac{1}{\tilde{v}_1}$ whenever $w_1 > w > 0$. In view of (2.3), we find that along S_1^c

$$\frac{dv}{dw} \ge -m := \min\{-c - \frac{1}{\tilde{v}_1}, \lambda_0^- - \delta\},\,$$

whenever 1 > w > 0. This leads to the second part of statement (i).

The first part of statement (ii) follows from Lemma 2.2 (ii). Since $c^* > c > 0$, there is no traveling wave and thus U_1^c and S_0^c do not intercept. This proves the statement (ii).

According to Lemma 2.2 (i), for v < 0, S_0^c lies below S_0^0 . On the other hand, since $c^* > c > 0$, S_0^c does not intercept U_1^c to form a heteroclinic orbit, and thus S_0^c lies above U_1^c . Consequently S_0^c intercepts the w-axis at a number w_1 between B and 1. Since the flow crosses the w-axis from above and since w' = v > 0 whenever v > 0, S_0^c lies on the left-hand side of line $w = w_1$ whenever v > 0. If S_0^c intersects with U_0^0 at a point (w_2, v_2) with $w_2 > 0$ and $v_2 > 0$, then $w_2 < B$. By Lemma 2.3 (i), U_0^0 is above S_0^c whenever w is between w_2 and w_1 . This leads to that U_0^0 is above the w-axis whenever w is between w_2 and w_1 , so that U_0^0 cannot intercept the w-axis at B. This contradiction shows that S_0^c does not intersect with U_0^0 whenever v > 0 and v > 0. We therefore conclude that S_0^c is above U_0^0 whenever v > 0, and thus S_0^c stays outside the loop determined by U_0^0 . Finally the uniqueness of solutions implies S_0^c does not intercept with S_1^c nor U_1^c , so that S_0^c lies below S_1^c , and S_0^c lies above U_1^c . This completes the proof of the statement (iii).

By Lemma 2.2 (i), U_0^c stays below S_0^0 and U_0^0 whenever v > 0. If U_0^c intercepts U_0^0 and S_0^0 below w-axis, we use (w_0, v_0) to denote the first point at which U_0^c intercepts U_0^0 and S_0^0 from above such that $v_0 < 0$ and U_0^c lies above U_0^0 and S_0^0 whenever v < 0 and $w > w_0$. On the other hand, by Lemma 2.3 (ii), U_0^c lies below S_0^0 whenever $w > w_0$ and v < 0. This leads to a contradiction. It follows that U_0^c stays inside the loop S_0^0 and U_0^0 for v > 0 and $v \le 0$. Since $g'(a) \ge 0$, (a, 0) is stable for c > 0. Furthermore for system (2.2),

$$\frac{dv}{dw} + \frac{d(-cv - g(w))}{dv} = -c < 0.$$

By Dulac's criterion, there is no limit cycle. It follows from the Poincaré-Bendixson Theorem that U_0^c approaches (a,0). The proof is complete.

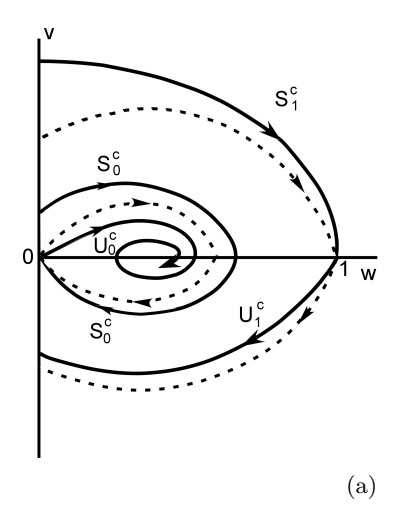
According to this lemma, S_1^c lies above S_0^c , and below a line v = -m(w-1) with m > 0. In view of the Poincaré-Bendixson Theorem, S_1^c must intersect the v-axis at a number $v_1 > 0$. Since S_0^c lies outside the loop S_0^0 and U_0^0 , below S_1^c , and above U_1^c , S_0^c must intersect the v-axis at a number $v_0 > 0$. See a graphical demonstration of the statements in Lemma 2.4 in Fig. 3 (a). Consider a trajectory T^c of (2.2) for $c^* > c > 0$ that starts at a number between v_0 and v_1 on the v-axis; see Fig. 3 (b) for a graphical description.

To study traveling waves for (1.1) and (1.2), we glue the phase portraits of (2.2) inside the patch to those outside the patch. Using phase plane analysis, we determine a critical patch size for the existence of traveling waves. Using z = x - ct and the substitution $u(x,t) = \bar{u}(z,t)$, (1.1) becomes

$$\bar{u}_t = \bar{u}_{zz} + c\bar{u}_z + f(\bar{u}, z).$$
 (2.6)

A traveling wave of (1.1) is a steady solution of (2.6) satisfying

$$w''(z) + cw'(z) + f(w, z) = 0, \quad z \in (-\infty, 0) \cup (0, L) \cup (L, \infty), \tag{2.7}$$



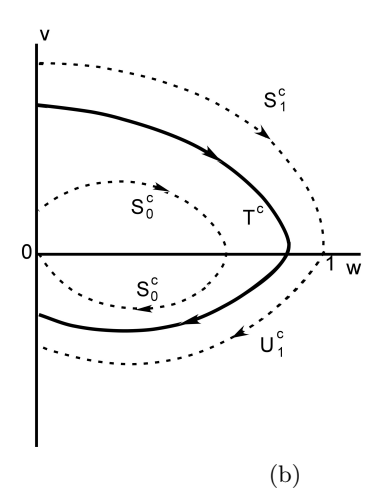


Figure 3: (a) The solid curves describe the stable and unstable manifolds S_0^c and U_0^c of (0,0) and stable and unstable manifolds S_1^c and U_1^c of (1,0) for 0 < w < 1 when $c^* > c > 0$. The dashed curves describe stable and unstable manifolds of (0,0) and (1,0) when c=0. (b) The solid curve describe an orbit T^c governed by (2.2) for 0 < w < 1 when $c^* > c > 0$. The dashed curves describe stable and unstable manifolds of (0,0) and (1,0) when $c^* > c > 0$.

187 with

$$w(0^+) = w(0^-), \ w(L^+) = w(L^-), \ w'(0^+) = w'(0^-), \ w'(L^+) = w'(L^-).$$
 (2.8)

188 The corresponding planar system is

$$w' = v, \quad 0 \le z \le L$$

 $v' = -cv - g(w), \quad 0 \le z \le L$ (2.9)

189 and

194

195

$$w' = v, \quad z < 0 \text{ or } z > L$$

 $v' = -cv + rw, \quad z < 0 \text{ or } z > L,$

$$(2.10)$$

with

$$w(0^+) = w(0^-), \ w(L^+) = w(L^-), \ v(0^+) = v(0^-), \ v(L^+) = v(L^-).$$

Throughout this paper we consider bounded traveling waves with values between 0 and 1. Bounded solutions with w > 0 for linear system (2.10) are given by

$$\begin{pmatrix} w \\ v \end{pmatrix} = k_1 e^{m^+ z} \begin{pmatrix} 1 \\ m^+ \end{pmatrix} \text{ for } z < 0; \qquad \begin{pmatrix} w \\ v \end{pmatrix} = k_1 e^{m^- z} \begin{pmatrix} 1 \\ m^- \end{pmatrix} \text{ for } z > L, \tag{2.11}$$

where $m^{\pm} = \frac{-c \pm \sqrt{c^2 + 4r}}{2}$, and k_1 and k_2 are positive constants. Here $w(-\infty) = w(\infty) = 0$. It follows that $v = m^+ w$ for z < 0 and $v = m^- w$ for z > L.

In the w-v plane, a bounded positive traveling wave described by (2.9) and (2.10) to a path involving $v=m^+w$, T^c (a trajectory of (2.2) or (2.9)), and $v=m^-w$. We use (w_0^c, v_0^c) and (w_1^c, v_1^c) to denote the interception points of S_0^c with line $v=m^+w$, and S_1^c with line $v=m^+w$, respectively. We use (p_1^c, q_1^c) and (p_2^c, q_2^c) to denote the interception points of T^c and line $v=m^+w$, and T^c and line

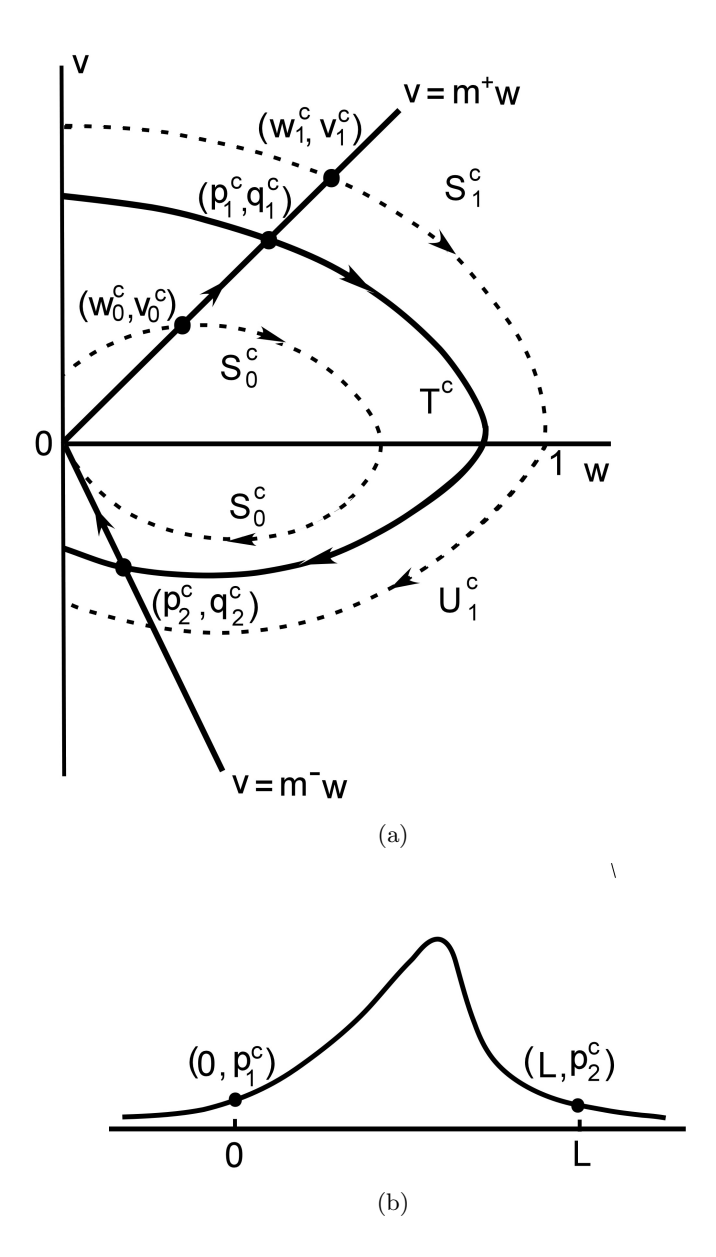


Figure 4: (a) A path for a positive traveling wave involving line $v = m^+w$, a trajectory T^c , and $v = m^-w$. (b) The corresponding traveling wave as a function of z = x - ct.

 $v = m^- w$, respectively. Note that $w_0^c < p_1^c < w_1^c$. See Fig. 4 (a) for a graphical description. The graph of the corresponding traveling wave is provided in Fig. 4 (b).

We now discuss how L is related to a traveling wave. In the first quadrant, by (2.9), w' = v > 0, so that w(x) increases in x and thus v can be viewed as a function of w. We use $v = v^+(p_1^c; w)$ to describe the upper part of T^c above the w-axis. Similarly v can be viewed as a function of w on T^c in the fourth quadrant. We use $v = v^-(p_1^c; w)$ to denote the lower part of T^c below the w-axis. We use w_*^c to denote the intersection of T^c and the w-axis. Observe $w_*^c > B > a$ so that $g(w_*^c) > 0$.

The first equation of (2.9) shows that L is given by

$$L = H(p_1^c) := \int_{p_1^c}^{w_*^c} \frac{1}{v^+(p_1^c; w)} dw + \int_{p_2^c}^{w_*^c} \frac{1}{-v^-(p_1^c; w)} dw.$$
 (2.12)

It should be noted that this is an improper integral due to $v^+(p_1^c, w)$ and $v^-(p_1^c, w)$ being zero at $w = w_*^c$.

Lemma 2.5. $H(p_1^c)$ is continuous in p_1^c for $p_1^c \in (w_0^c, w_1^c)$.

Proof. Since $g(w) \in C^1[0,1]$, the solution (w(z),v(z)) along T^c continuously depends on the initial values $w(0) = p_1^c$ and $v(0) = m^+p_1^c$ and thus on p_1^c (see Theorem 1.3.1 in [14]). Consequently, $p_2^c = w(L)$ and $q_2^c = v(L) = m^-p_2^c$ continuously depend on p_1^c . Along $v = v^+(p_1^c; w) > 0$, the first equation of (2.9) shows $\frac{dw}{dz} > 0$, so that w(z) is strictly increasing and thus x is a continuous function of w. We conclude that $v^+(p_1^c; w)$ is a continuous function of w for $p_1^c \le w \le w_*^c$. Similarly, $v^-(p_1^c; w)$ is a continuous function of w for $p_2^c \le w \le w_*^c$.

In view of (2.9), near $(w_*^c, 0)$, $v' \cong -g(w_*^c) < 0$, so that w is a function of v on T^c . Furthermore,

$$\frac{dw(v)}{dv}|_{v=0} = -\frac{v}{cv + g(w)}|_{w=w_*^c, v=0} = -\frac{0}{g(w_*^c)} = 0,$$

and

205

$$\frac{d^2w(v)}{dv^2}|_{v=0} = -\frac{cv + g(w) - v(c + g'(w)\frac{dw}{dv})}{[cv + g(w)]^2}|_{w=w_*^c, v=0} = -\frac{1}{g(w_*^c)} < 0.$$

It follows that for any small $\epsilon > 0$, there exists $\gamma > 0$ such that for $w \in [w_*^c - \gamma, w_*^c], w > w_*^c + (-\frac{1}{g(w_*^c)} - \frac{1}{g(w_*^c)})$ so that

$$\frac{1}{|v|} < \sqrt{\left(\frac{1}{g(w_*^c)} + \epsilon\right) \frac{1}{w_*^c - w}}.$$
 (2.13)

This particularly is true when v is replaced by $v^{\pm}(p_1^c; w)$. Therefore $H(p_1^c)$ given by (2.12) is well-defined.

Consider a trajectory \tilde{T}^c of (2.9) with \tilde{p}_1^c as the w-coordinate of the intersection point with $v=m^+w$, \tilde{p}_2^c as the w-coordinate of the intersection point with $v=m^-w$, and \tilde{w}_*^c as the w-intercept. Assume $w_1^c > p_1^c > \tilde{p}_1^c > w_0^c$. Lemma 2.3 (i) shows that T^c is above \tilde{T}^c for v>0, and consequently $w_*^c > \tilde{w}_*^c$. For any small $\varepsilon>0$, continuity and (2.13) imply that there exists $\delta_1>0$ such that for $p_1^c-\tilde{p}_1^c<\delta_1$,

$$\int_{\tilde{w}_*^c}^{w_*^c} \frac{1}{v^+(p_1^c; w)} dw < \frac{\varepsilon}{3}.$$
 (2.14)

Use $\tilde{v}^+(\tilde{p}_1^c;w)$ ($\tilde{v}^-(\tilde{p}_1^c;w)$) to denote the part of \tilde{T}_c above (below) the w-axis. Choose w_0 with $p_1^c < w_0 < \tilde{w}_*^c$ and w_0 sufficiently close to \tilde{w}_*^c , such that

$$\int_{w_0}^{\tilde{w}_*^c} \frac{1}{\tilde{v}^+(\tilde{p}_1^c; w)} dw < \frac{\varepsilon}{3}, \tag{2.15}$$

and $\tilde{v}^+(\tilde{p}_1^c;w) \geq \tilde{v}^+(\tilde{p}_1^c;w_0)$ for $\tilde{p}_1^c \leq w \leq w_0$. For $\delta_2 = \tilde{v}^+(\tilde{p}_1^c;w_0)\frac{\varepsilon}{3}$ and $p_1^c - \tilde{p}_1^c < \delta_2$,

$$\int_{\tilde{p}_{1}^{c}}^{p_{1}^{c}} \frac{1}{\tilde{v}^{+}(\tilde{p}_{1}^{c}; w)} dw \le \frac{p_{1}^{c} - \tilde{p}_{1}^{c}}{\tilde{v}^{+}(\tilde{p}_{1}^{c}; w_{0})} < \frac{\varepsilon}{3}.$$
(2.16)

Let $S = v^+(p_1^c; w) - \tilde{v}^+(\tilde{p}_1^c; w)$ for $w \in [p_1^c, w_0] \subset [0, 1]$. The equation (2.3) shows that

$$S' = -\frac{g(w)}{v^{+}(p_1^c; w)\tilde{v}^{+}(\tilde{p}_1^c; w)}S.$$

In view of this and $\tilde{v}^+(\tilde{p}_1^c; w) < v^+(p_1^c; w)$ for w > 0, we have for $w \in [p_1^c, w_0]$,

$$S(w) = S(p_1^c) e^{-\int_{p_1^c}^w \frac{g(\xi)}{v^+(p_1^c;\xi)\overline{v}^+(\bar{p}_1^c;\xi)} d\xi} \le S(p_1^c) e^{-(w-p_1^c)\frac{g_-}{(\bar{v}^+(\bar{p}_1^c;w_0))^2}} \le (v^+(p_1^c;p_1^c) - \bar{v}^+(\bar{p}_1^c;p_1^c)) e^{-\frac{g_-}{(\bar{v}^+(\bar{p}_1^c;w_0))^2}},$$

where $g_{-} < 0$ is the minimal value of g(w) for $w \in [0, 1]$. We therefore have that

$$\begin{split} &\int_{p_{1}^{c}}^{w_{0}} (\frac{1}{\tilde{v}^{+}(\tilde{p}_{1}^{c};w)} - \frac{1}{v^{+}(p_{1}^{c};w)}) dw \\ &= \int_{p_{1}^{c}}^{w_{0}} \frac{v^{+}(p_{1}^{c};w) - \tilde{v}^{+}(\tilde{p}_{1}^{c};w)}{v^{+}(p_{1}^{c};w)\tilde{v}^{+}(\tilde{p}_{1}^{c};w)} dw \\ &\leq (w_{0} - p_{1}^{c}) \frac{v^{+}(p_{1}^{c};p_{1}^{c}) - \tilde{v}^{+}(\tilde{p}_{1}^{c};p_{1}^{c})}{(\tilde{v}^{+}(\tilde{p}_{1}^{c};w_{0}))^{2}} e^{-\frac{g_{-}}{(\tilde{v}^{+}(\tilde{p}_{1}^{c};w_{0}))^{2}}} \\ &\leq \frac{v^{+}(p_{1}^{c};p_{1}^{c}) - \tilde{v}^{+}(\tilde{p}_{1}^{c};p_{1}^{c})}{(\tilde{v}^{+}(\tilde{p}_{1}^{c};w_{0}))^{2}} e^{-\frac{g_{-}}{(\tilde{v}^{+}(\tilde{p}_{1}^{c};w_{0}))^{2}}}. \end{split}$$

Since $v^+(p_1^c; p_1^c) - \tilde{v}^+(\tilde{p}_1^c; p_1^c)$ approaches 0 as p_1^c approaches \tilde{p}_1^c , there exists $\delta_3 > 0$ such that for $p_1^c - \tilde{p}_1^c < \delta_3$,

$$\int_{p_1^c}^{w_0} \left(\frac{1}{\tilde{v}^+(\tilde{p}_1^c; w)} - \frac{1}{v^+(p_1^c; w)} \right) dw < \frac{\varepsilon}{3}. \tag{2.17}$$

Combining (2.14)-(2.17), we obtain that for $p_1^c - \tilde{p}_1^c < \delta$ with $\delta = \min_{1 \le i \le 3} {\{\delta_i\}}$,

$$\left| \int_{p_1^c}^{w_*^c} \frac{1}{v^+(p_1^c; w)} dw - \int_{\tilde{p}_1^c}^{\tilde{w}_*^c} \frac{1}{\tilde{v}^+(\tilde{p}_1^c; w)} dw \right| < \varepsilon.$$

Similarly, for the given ε , there exists $\hat{\delta} > 0$ such that for $p_1^c - \tilde{p}_1^c < \hat{\delta}$,

$$\left| \int_{p_2^c}^{w_*^c} \frac{1}{v^-(p_1^c; w)} dw - \int_{\tilde{p}_2^c}^{\tilde{w}_*^c} \frac{1}{\tilde{v}^-(\tilde{p}_1^c; w)} dw \right| < \varepsilon.$$

We have shown that $H(p_1^c)$ is a continuous function of p_1^c . The proof is complete.

Lemma 2.6. Assume that Hypotheses 2.1 hold and $c^* > c > 0$. Then $H(p_1^c)$ given by (2.12) satisfies $\lim_{p_1^c \to w_0^{c+}} H(p_1^c) = \infty$ and $\lim_{p_1^c \to w_0^{c-}} H(p_1^c) = \infty$.

Proof. The tangent line to S_1^c at (1,0) is $v = \lambda_1^-(w-1)$ with $\lambda_1^- = -\frac{\sqrt{c^2 - 4g'(1)} + c}{2} < 0$. For any small number $\delta > 0$, there exists a number $w_1 < 1$ and w_1 close to 1 such that S_1^c lies below $v = (\lambda_1^- - \delta)(w-1)$ for $w_1 \le w < 1$. Consider a trajectory T^c of (2.9) close to S_1^c near (1,0) with w_*^c , the w-intercept satisfying $w_1 < w_*^c < 1$. Since T^c lies below S_1^c , T^c has a point with w_1 as the w-coordinate. Since T^c lies below $v = (\lambda_1^- - \delta)(w-1)$ for $w_1 \le w < 1$, (2.12) shows

$$H(p_1^c) \ge \int_{w_1}^{w_*^c} \frac{1}{v^+(p_1^c; w)} dw \ge \int_{w_1}^{w_*^c} \frac{1}{(\lambda_1^- - \delta)(w - 1)} dw.$$

This shows $H(p_1^c) \to \infty$ as w_*^c approaches 1 from the left. Due to continuous dependence of a solution on its initial value, $w_*^c \to 1$ from the left if $p_1^c \to w_1^c$ from the left. We therefore have $H(p_1^c) \to \infty$ as $p_1^c \to w_1^{c-}$.

The tangent line to S_0^c at (0,0) is $v=\lambda_0^-w$ with $\lambda_0^-=-\frac{\sqrt{c^2-4g'(0)}+c}{2}<0$. For any small positive number δ with $\delta<|\lambda_0^-|$, there exists a point (w_0,v_0) on S_0^c close to (0,0) with $0< w_0< a$ and $v_0<0$ such that S_0^c lies below the line $v=(\lambda_0^-+\delta)w$ for $0< w\leq w_0$, and $g(w)>(g'(0)-\delta)w$ for $0< w\leq w_0$. Consider a trajectory T^c of (2.9) close to S_0^c near (0,0) with $p_2^c< w_0$ and $q_2^c>v_0$. Since T^c is below S_0^c for v<0, T^c has a point (w_0,v_1) with v<0, $v_1< v_0$. In view of (2.3), along T^c for $p_2^c\leq w\leq w_0$,

$$\frac{dv^{-}}{dw} = -c - \frac{g(w)}{v^{-}} < -c < 0,$$

so that $v^-(p_1^c; w)$ is a decreasing function in w. Since T^c lies below S_0^c near (0,0), T^c lies below the line $v = (\lambda_0^c + \delta)w$ for $q_2^c > v \ge v_0$. We therefore use (2.12), a variable change, and (2.3) to obtain

$$H(p_1^c) \ge \int_{p_2^c}^{w_0} \frac{1}{-v^-(p_1^c;w)} dw = \int_{q_2^c}^{v_1} \frac{1}{-v^-} \frac{1}{-c-g(w)/v^-} dv^- = \int_{v_1}^{q_2^c} \frac{1}{-cv^--g(w)} dv^-$$

$$\ge \int_{v_0}^{q_2^c} \frac{1}{-cv^--(g'(0)-\delta)w} dv^- \ge \int_{v_0}^{q_2^c} \frac{1}{\left(-c-\frac{g'(0)-\delta}{\lambda_0^-+\delta}\right)v^-} dv^-.$$

This shows that $H(p_1^c) \to \infty$ as $q_2^c \to 0^+$. Due to continuous dependence of a solution on its initial value, $q_2^c \to 0^+$ if $p_1^c \to w_0^{c+}$. This completes the proof.

233 Define

$$L^*(c) = \inf_{w_0^c < p_1^c < w_1^c} H(p_1^c), \tag{2.18}$$

where $H(p_1^c)$ is given by (2.12). Lemma 2.5 and Lemma 2.6 show that $L^*(c)$ is well-defined. Clearly, $L^*(c) \geq 0$. Ecologically speaking, $L^*(c)$ is the critical patch size for a population to persist. We will further explore $L^*(c)$ in the rest of this section.

We shall show that $L^*(c)$ is positive. To this end, we introduce an integral operator. Integral operators have been proven useful in studying traveling waves for reaction-diffusion systems [23]. Consider Q_c defined by

$$Q_c[u](z) := \int_{-\infty}^{\infty} m_c(z-y) \frac{f(u(y), y) + \rho u(y)}{\rho} dy,$$

with

$$m_c(z) = \frac{\rho}{\sqrt{c^2 + 4\rho}} \begin{cases} e^{-\lambda_1 z} & \text{if } z \ge 0, \\ e^{\lambda_2 z} & \text{if } z < 0, \end{cases}$$

where $\lambda_1 = \frac{1}{2}(\sqrt{c^2 + 4\rho} + c) > 0$, $\lambda_2 = \frac{1}{2}(\sqrt{c^2 + 4\rho} - c) > 0$, and ρ is a positive constant satisfying $\rho > \max_{u \in [0,1]} |g'(u)|$ and $\rho > r$. It is easily seen that $m_c(z)$ is a probability density function, that is, $m_c(z) > 0$ and $\int_{-\infty}^{\infty} m_c(z) dz = 1$. Since $\frac{f(u,y) + \rho u}{\rho}$ is increasing in u, Q_c is a monotone operator.

The next lemma shows that w(x-ct) is a bounded traveling wave of (1.1) if and only if w is a fixed point of Q_c .

Lemma 2.7. Assume that Hypotheses 2.1 hold. Then w satisfies (2.7) and (2.8) with $w(-\infty)=w(\infty)=0$ if and only if w(z) is a fixed point of Q_c (i.e., $w(z)=Q_c[w](z)$) with $w(-\infty)=w(\infty)=0$.

If w satisfies (2.7) and (2.8) with $w(-\infty) = w(\infty) = 0$, a slightly revised version of the first part of the proof Theorem 3.2 in [23] shows that w(z) is a fixed point of Q_c . If w(z) is a fixed point of Q_c with $w(-\infty) = w(\infty) = 0$, a proof similar to that of Lemma 3.1 in [27] and the second part of Theorem 3.2 in [23] show that w satisfies (2.7) and (2.8). We omit the details here.

Lemma 2.8. Assume that Hypotheses 2.1 hold and $c^* > c \ge 0$. Then there exists a positive number $L_0(c)$ such that for $L < L_0(c)$, there is no positive traveling wave connecting 0 and 0 for (1.1).

 $_{250}$ *Proof.* We consider

$$w_{n+1}(z) = Q_c[w_n](z), \quad w_0(z) \equiv 1.$$
 (2.19)

Since Q_c is monotone, $w_1(z) = \int_{-\infty}^{\infty} m_c(z-y) \frac{f(w_0(y),y) + \rho w_0(y)}{\rho} dy = \int_{-\infty}^{\infty} m_c(z-y) \frac{f(1,y) + \rho}{\rho} dy \le \int_{-\infty}^{\infty} m_c(z-y) \frac{f($

Let $\bar{w}_n = \sup_{-\infty < z < \infty} w_n(z)$. If follows from (2.19) that

$$w_{n+1}(z) \le Q_c[\bar{w}_n](z) := \frac{\rho}{\sqrt{c^2 + 4\rho}} \Big\{ \int_{-\infty}^z e^{-\lambda_1(z-y)} \frac{f(\bar{w}_n, y) + \rho \bar{w}_n}{\rho} dy + \int_x^\infty e^{\lambda_2(z-y)} \frac{f(\bar{w}_n, y) + \rho \bar{w}_n}{\rho} dy \Big\}.$$

For $z \leq 0$,

$$Q_{c}[\bar{w}_{n}](z) = \frac{\rho}{\sqrt{c^{2}+4\rho}} \left\{ e^{-\lambda_{1}z} \int_{-\infty}^{z} e^{\lambda_{1}y} \frac{\rho-r}{\rho} \bar{w}_{n} dy + e^{\lambda_{2}z} \int_{z}^{0} e^{-\lambda_{2}y} \frac{\rho-r}{\rho} \bar{w}_{n} dy + e^{\lambda_{2}z} \int_{0}^{L} e^{-\lambda_{2}y} \frac{g(\bar{w}_{n})+\rho\bar{w}_{n}}{\rho} dy + e^{\lambda_{2}z} \int_{L}^{\infty} e^{-\lambda_{2}y} \frac{\rho-r}{\rho} \bar{w}_{n} dy \right\}$$

$$\leq \frac{\rho}{\sqrt{c^{2}+4\rho}} \left\{ \frac{\rho-r}{\rho} \left[\frac{1}{\lambda_{1}} + \frac{1-e^{\lambda_{2}z}+e^{\lambda_{2}(z-L)}}{\lambda_{2}} \right] + \frac{2}{\lambda_{2}} (1-e^{-\lambda_{2}L}) e^{\lambda_{2}z} \right\} \bar{w}_{n}.$$

Here we have used the simple fact $\frac{g(\bar{w}_n) + \rho \bar{w}_n}{\rho} \leq 2\bar{w}_n$. For $z \leq 0$, $e^{\lambda_2 z} \leq 1$, $0 < 1 - e^{\lambda_2 z} + e^{\lambda_2 (z - L)} < 1$.

We therefore have for $z \leq 0$,

$$Q_{c}[\bar{w}_{n}](z) \leq \frac{\rho}{\sqrt{c^{2} + 4\rho}} \left\{ \frac{\rho - r}{\rho} \left[\frac{1}{\lambda_{1}} + \frac{1}{\lambda_{2}} \right] + \frac{2}{\lambda_{2}} (1 - e^{-\lambda_{2}L}) \right\} \bar{w}_{n}.$$
 (2.20)

For 0 < z < L,

$$Q_{c}[\bar{w}_{n}](z) = \frac{\rho}{\sqrt{c^{2}+4\rho}} \left\{ e^{-\lambda_{1}z} \int_{-\infty}^{0} e^{\lambda_{1}y} \frac{\rho-r}{\rho} \bar{w}_{n} dy + e^{-\lambda_{1}z} \int_{0}^{z} e^{\lambda_{1}y} \frac{g(\bar{w}_{n})+\rho\bar{w}_{n}}{\rho} dy + e^{\lambda_{2}z} \int_{z}^{L} e^{-\lambda_{2}y} \frac{g(\bar{w}_{n})+\rho\bar{w}_{n}}{\rho} dy + e^{\lambda_{2}z} \int_{L}^{\infty} e^{-\lambda_{2}y} \frac{\rho-r}{\rho} \bar{w}_{n} dy \right\}$$

$$\leq \frac{\rho}{\sqrt{c^{2}+4\rho}} \left\{ \frac{\rho-r}{\rho} \left[\frac{e^{-\lambda_{1}z}}{\lambda_{1}} + \frac{e^{\lambda_{2}(z-L)}}{\lambda_{2}} \right] + \frac{2}{\lambda_{1}} (1 - e^{-\lambda_{1}z}) + \frac{2}{\lambda_{2}} (1 - e^{\lambda_{1}(z-L)}) \right\} \bar{w}_{n}$$

$$\leq \frac{\rho}{\sqrt{c^{2}+4\rho}} \left\{ \frac{\rho-r}{\rho} \left[\frac{1}{\lambda_{1}} + \frac{1}{\lambda_{2}} \right] + \frac{2}{\lambda_{1}} (1 - e^{-\lambda_{1}L}) + \frac{2}{\lambda_{2}} (1 - e^{-\lambda_{2}L}) \right\} \bar{w}_{n}.$$

$$(2.21)$$

For z > L,

$$Q_{c}[\bar{w}_{n}](z) = \frac{\rho}{\sqrt{c^{2}+4\rho}} \left\{ e^{-\lambda_{1}z} \int_{-\infty}^{0} e^{\lambda_{1}y} \frac{\rho-r}{\rho} \bar{w}_{n} dy + e^{-\lambda_{1}z} \int_{0}^{L} e^{\lambda_{1}y} \frac{g(\bar{w}_{n})+\rho\bar{w}_{n}}{\rho} dy + e^{-\lambda_{1}z} \int_{L}^{z} e^{\lambda_{1}y} \frac{\rho-r}{\rho} \bar{w}_{n} dy + e^{-\lambda_{1}z} \int_{L}^{z} e^{\lambda_{1}y} \frac{\rho-r}{\rho} \bar{w}_{n} dy \right\}$$

$$\leq \frac{\rho}{\sqrt{c^{2}+4\rho}} \left\{ \frac{\rho-r}{\rho} \left[\frac{1-e^{-\lambda_{1}(z-L)}+e^{-\lambda_{1}z}}{\lambda_{1}} + \frac{1}{\lambda_{2}} \right] + \frac{2}{\lambda_{1}} (e^{\lambda_{1}L} - 1)e^{-\lambda_{1}z} \right\} \bar{w}_{n}$$

$$\leq \frac{\rho}{\sqrt{c^{2}+4\rho}} \left\{ \frac{\rho-r}{\rho} \left[\frac{1}{\lambda_{1}} + \frac{1}{\lambda_{2}} \right] + \frac{2}{\lambda_{1}} (e^{\lambda_{1}L} - 1) \right\} \bar{w}_{n}.$$

$$(2.22)$$

Observe $\frac{\rho}{\sqrt{c^2+4\rho}}[\frac{1}{\lambda_1}+\frac{1}{\lambda_2}]=1$. Since $\frac{\rho-r}{\rho}<1$, (2.20)-(2.22) show that there exist positive numbers $\sigma<1$ and $L_0(c)$ such that for $L\leq L_0(c)$ and any $z,\,w_{n+1}(z)\leq\sigma\bar{w}_n$ leading to $\bar{w}_{n+1}\leq\sigma\bar{w}_n$. Therefore for $L\leq L_0(c)$, $\bar{w}_n\to 0$ as $n\to\infty$. We conclude that for $L\leq L_0(c)$, the solution $w_n(z)$ of (2.19) approaches 0 as $n\to\infty$. This and Lemma 2.7 imply that for $L\leq L_0(c)$, system (1.1) has no positive traveling wave. The proof is complete.

Theorem 2.1. Assume that Hypotheses 2.1 hold. Let $\int_0^1 g(u) > 0$. Then for $c^* > c > 0$ and $L^*(c)$ defined by (2.18),

- i. $L^*(c) > 0$;
- ii. If $L = L^*(c)$, equation (1.1) has a positive traveling wave connecting 0 and 0;
- 266 iii. If $L > L^*(c)$, equation (1.1) has two positive traveling waves connecting 0 and 0; and
- iv. If $L < L^*(c)$, equation (1.1) has no positive traveling wave connecting 0 and 0.

Proof. By Lemma 2.5 and Lemma 2.6, $L^*(c)$, the infinum of $H(p_1^c)$ occurs at a number between w_0^c and w_1^c , so that there is a corresponding traveling wave. For $L > L^*(c)$, there exists two different numbers in (w_0^c, w_1^c) at which H has the value L, and thus there exist two positive corresponding traveling waves. These prove (ii) and (iii). On the other hand, a positive traveling wave corresponds to the existence of $p_1^c \in (w_0^c, w_1^c)$ such that $L = H(p_1^c)$. Consequently if $L^*(c) > 0$, for $0 < L < L^*(c)$ there is no positive traveling wave. Lemma 2.8 shows that there exists $L_0(c) > 0$ such that for $L < L_0(c)$ there is no positive traveling wave. If follows that $L^*(c) \ge L_0(c)$. These prove (i) and (iv). The proof is complete.

The statements (ii) and (iii) of this theorem show the existence of one or two positive traveling waves. The problem of exact number of positive traveling waves is open. Our numerical simulations in the next section indicate that for g(u) in the form of u(u-a)(1-u) and for $L > L^*(c)$, there are exactly two positive traveling waves.

Theorem 2.2. Assume that Hypotheses 2.1 hold. If either (i) $\int_0^1 g(u)du > 0$ and $c > c^*$, or (ii) $\int_0^1 g(u)du < 0$ and $c \ge 0$, then for any L > 0 equation (1.1) has no positive traveling wave connecting 0 and 0.

Proof. Assume that w(x-ct) is a traveling wave connecting 0 and 0 for (1.1) and (1.2) in the case of $\int_0^1 g(u)du > 0$ and $c > c^* > 0$. Since $0 \le w(x) \le 1$ and $0 \le \frac{f(w(x),x) + \rho w(x)}{\rho} \le 1$ for all x, and since $0 \le \frac{f(w(x),x) + \rho w(x)}{\rho} = \frac{\rho - r}{\rho} w(x) \le \frac{\rho - r}{\rho} < 1$, $w(x) = Q_c[w](x)$ implies that $0 \le w(x) < 1$ for all x. Since $w(\infty) = w(-\infty) = 0$, there exists a positive number $\gamma < 1$ such that

$$0 \le w(x) \le \gamma,\tag{2.23}$$

for all x. $w(x) = k_1 e^{m^- x}$ for x > 0, where k_1 is a positive number and $m^- = \frac{-c - \sqrt{c^2 + 4r}}{2} < 0$.

Consider the nonincreasing traveling wave $w^*(x-c^*t)$ for (2.1) with $w^*(-\infty)=1$ and $w^*(\infty)=0$ described by Proposition 2.1. This traveling wave corresponds the orbit T^* from (1,0) to (0,0) in the w-v plane. We use $v=h(w^*)$ to describe this orbit. The tangent line to $v=h(w^*)$ at (0,0) is $v=\lambda_0^-w^*$

where $\lambda_0^- = \frac{-c^* - \sqrt{(c^*)^2 - 4g'(0)}}{2} < 0$. Since r > -g'(0) and $c > c^*$, for $\lambda_0^- - m^- > \epsilon > 0$, there exists $\delta > 0$ such that $h(w^*) \geq (\lambda_0^- - \epsilon)w^*$ for $\delta > w^* > 0$. This and the first equation of (2.2) show that there exists x_0 such that for $x > x_0$,

$$(w^*)' \geq (\lambda_0^- - \epsilon)w^*,$$

leading to $w^*(x) \ge k_0 e^{(\lambda_0^- - \epsilon)x}$ for $x > x_0$ and some $k_0 > 0$. This, $w(z) = k_1 e^{m^- x}$ for x > 0, (2.23), and $w^*(-\infty) = 1$ show that there is a real number d such that $w^*(x+d) > w(x)$ for $-\infty < x < \infty$. Since $g(u) \ge f(u,x)$, comparison shows that $w^*(x+d-c^*t) \ge w(x-ct)$ for all t > 0 and $-\infty < x < \infty$. If $w(x_1) > 0$ for some real number x_1 , there exists x_2 such that $x_2 - d > x_1$ and $w^*(x_2) < w(x_1)$. For $t_1 = \frac{x_2 - d - x_1}{c - c^*} > 0$ and $t_2 = x_1 + ct_1$, $t_2 = x_2 + ct_2$, $t_3 = x_1 + ct_3$, $t_4 = x_3 + ct_4$, $t_5 = x_4 + ct_5$, $t_5 = x_5 + ct_5$. We conclude $t_5 = x_5 + ct_5$. We have shown when $t_5 = x_5 + ct_5$ and $t_5 = x_5 + ct_5$ for any $t_5 = x_5 + ct_5$. The proof for the case of $t_5 = x_5 + ct_5$ for any $t_5 = x_5 + ct_5$ has no positive traveling wave. The proof for the case of $t_5 = x_5 + ct_5$ for any $t_5 = x_5 + ct_5$ has no positive traveling wave. The proof for the case of $t_5 = x_5 + ct_5$ for any $t_5 = x_5 + ct_5$ has no positive traveling wave. The proof for the case of $t_5 = x_5 + ct_5$ for any $t_5 = x_5 + ct_5$ has no positive traveling wave. The proof for the case of $t_5 = x_5 + ct_5$ for any $t_5 = x_5 + ct_5$ for any $t_5 = x_5 + ct_5$ has no positive traveling wave. The proof for the case of $t_5 = x_5 + ct_5$ for any $t_5 = x_5 + ct_5$ has no positive traveling wave. The proof for the case of $t_5 = x_5 + ct_5$ for any $t_5 = x_5 +$

3 Simulations

In these simulations we first numerically study the phase plane equations given by (2.9) and (2.10). We will also numerically study the fully time dependant solutions to (1.1) and (1.2). Throughout this section we will use g(u) = u(u - a)(1 - u), therefore the dynamics are characterized by the parameters a, c, r and L. For simplicity, we use L^* to denote $L^*(c)$ for a given c.

In Fig. 5 we integrate the phase plane equations for the parameters a=0.2, r=1, and $c=0.5c^*=0.212$. We use MATLAB's ode45 to accomplish the integration. For this choice of parameters $(w_0^c, v_0^c)=(0.185, 0.167)$ and $(w_1^c, v_1^c)=(0.424, 0.381)$. This was determined by backwards integration of the equations with initial conditions $(0.001, 0.001m^-)$ and (1, 0.001) respectively. The intersection with $v=m^+w$ was determined by using the odeset 'Events' option to terminate integration.

To create Fig. 5-(b) we forward integrate trajectories initiated along the line segment connecting (w_0^c, v_0^c) and (w_1^c, v_1^c) . The initial point is related to β by $w = (1-\beta)w_0^c + \beta w_1^c$ and $v = (1-\beta)v_0^c + \beta v_1^c$. To determine the length of the habitat corresponding to the solution we used 'Events' to terminate integration when the intersection with $v = m^- w$ is detected. The returned value of the independent variable is the length. We see there is a broad minima approximately near $\beta = 0.6$ and L = 7 with L asymptotically approaching infinity as β approaches 0 and 1. The exact values of the minima (as determined by the minima of the 500 sample points) is $\beta = 0.611$ and $L^* = 6.790$. The values of β corresponding to L = 8 are $\beta = 0.197$ and $\beta = 0.923$ as determined by linear interpolation. The trajectories are plotted Fig. 5-(a). The corresponding travelling waves are plotted in Fig. 6.

In Fig. 7 we show the relation between L^* and the habitat shift speed relative to c^* . In Fig. 7-(a) r=1 and several different value of a are displayed. We see that for a fixed c the minimum habitat size increases as a increases. Since a smaller of a means stronger growth, this is not surprising. In Fig. 7-(b) a=0.2 and several different value of r are displayed. As a larger r means faster die off in the bad habitat, we see the minimum habitat size increases with r. We also see that L^* increases very gradually with c until roughly 80% of c^* where it begins increasing more rapidly. Due to the limits of numerical accuracy, L^* was only computed up to $c=0.99c^*$. To compute L^* , L versus β was computed as in Fig. 5-(b) for 250 sample points on the interval $0.01 \le \beta \le 0.99$. The minimum of these values was assigned to L^* .

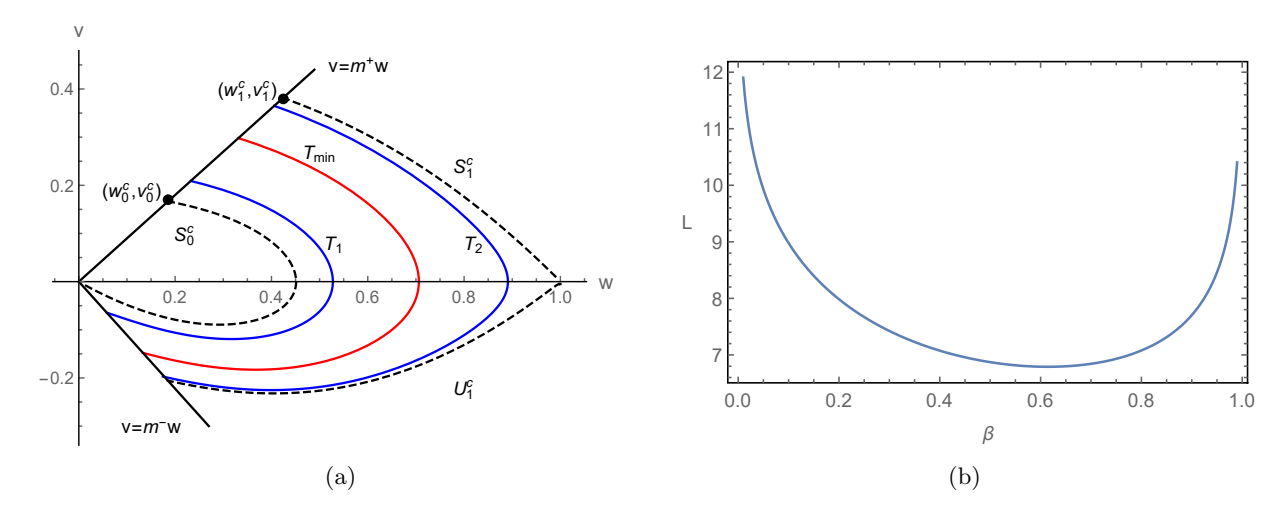


Figure 5: In (a) several phase plane trajectories for the parameters $a=0.2,\ r=1,\ c=0.5c^*$ are shown. The blue curves $(T_1 \text{ and } T_2)$ correspond to the solutions with L=8, and the red curve (T_{\min}) is the trajectory corresponding to the minimum habitat size, L^* , which is 6.79. In (b) we show how habitat length varies with β . β defines the initial point via $w=(1-\beta)w_0^c+\beta w_1^c$ and $v=(1-\beta)v_0^c+\beta v_1^c$.

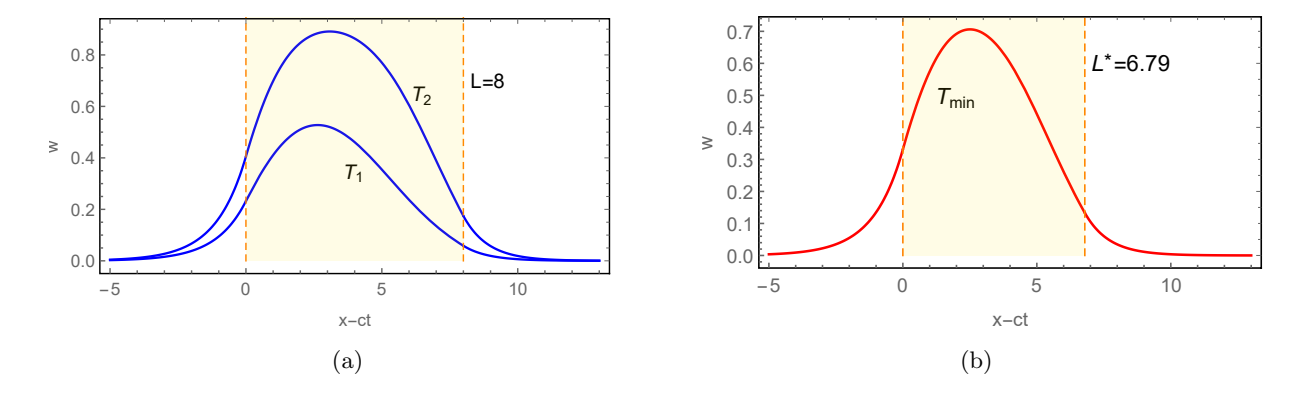


Figure 6: The travelling waves corresponding to the trajectories in Fig. 5.

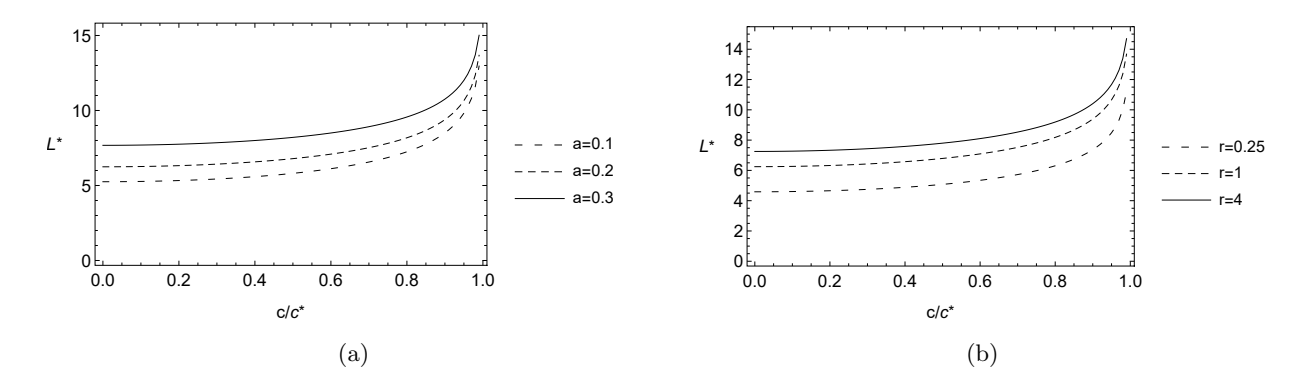


Figure 7: We show the minimum habitat size, L^* , as a function of the habitat shift speed relative to c^* . In (a) r is 1 and the curves for several values of a are shown. In (b) a is 0.2 and the curves for several values of r are shown.

In figures 8-10 we examine the evolution of the fully time dependant solutions. To avoid complications of dynamically updating the effectively populated domain, we use the moving frame equation given by (2.6).

To numerically approximate the equation we used uniform spatial sampling with $\delta z = 0.2$ or the nearest number that insures a whole number of sample points in the interval [0, L]. The first and second derivatives are interpolated up to fourth order in δx . To deal with the discontinuity in the second derivative at z = 0 and z = L, the boundary conditions that u and u_z are continuous there is applied and appropriate end-point interpolations are used. The domain was extended to the left (right) of z = 0 (z = L) by 25 units and the boundary condition u = 0 was applied at the end-points. A fixed time step $\delta t = 0.006$ with a second order Runge-Kutta method is used for time integration. Larger values of δt , such as $\delta t = 0.1$, exhibited unstable oscillations consistent with a stiff-system. In future updates to this code, it may be desirable to implement an implicit solver such as Backward-Euler or Crank-Nicolson. The code used can be viewed at

https://github.com/glotto01/Reaction_Diffusion.git

In Fig. 8 and 9 we show the dynamics of a solution where $L > L^*$. We use the same parameters as in Fig. 6-(a). Namely, a = 0.2, r = 1, $c = 0.5c^*$ and L = 8. In Fig. 8-(a) we see that a solution converges from above to the T_2 equilibrium. The initial condition used is u(x,0) = 1. In Fig. 8-(b) we see a solution converge from below to the T_2 equilibrium. The initial condition used is $u(x,0) = 0.6e^{-0.1(x-4)^2}$. The black dashed curve is the T_2 equilibrium as computed from the phase-plane equations. Qualitatively similar dynamics where seen with other parameter choices when $L > L^*$.

In Fig. 9 we numerically examine the stability of the T_1 equilibrium. In (a) we initiate with $u(x,0) = 1.05T_1(x)$. We see that the solution asymptotically approaches the T_2 equilibrium. In (b) we initiate with $u(x,0) = 0.95T_1(x)$. We see that the solution asymptotically approaches zero. This strongly suggests that T_1 acts as a separatrix, where solutions initiated below it go extinct, and solutions initiated above it grow to the T_2 equilibrium. Similar results were seen with other parameter choices.

In Fig. 10 we show an example of extinction occurring when $L < L^*$ and when $c > c^*$. In Fig. 10-(a) the habitat size used is L = 6 which is less than L^* which is 6.79 for the parameters used $(c = 0.5c^*, a = 0.2, r = 1)$. The initial condition used is u(x, 0) = 1. We see by t = 38 the maximum

density has fallen below the Allee threshold of 0.2. In Fig. 10-(b), $c = 1.2c^*$ so the habitat shift speed is greater then species spread speed and by the theory developed we would expect even for large values of L extinction will eventually occur. We use the parameters a = 0.2, r = 1 and L = 10. We see that by t = 55 the maximum density has already fallen below the Allee threshold.

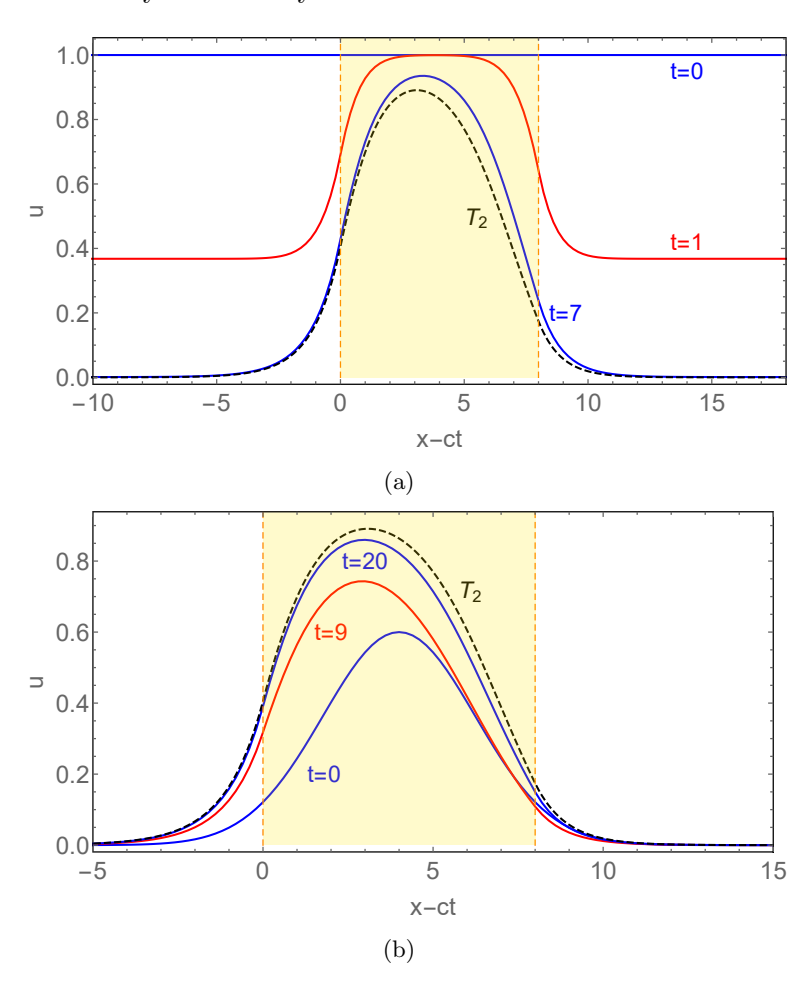


Figure 8: Time dependent solutions for the parameters $c=0.5c^*$, a=0.2, r=1, and L=8. In (a) we see that the solution converges to the T_2 equilibrium from above. The initial condition used was u(x,0)=1. In (b) we see the solution converges to the T_2 equilibrium from below. The initial condition used was $u(x,0)=0.6e^{-0.1(x-4)^2}$.

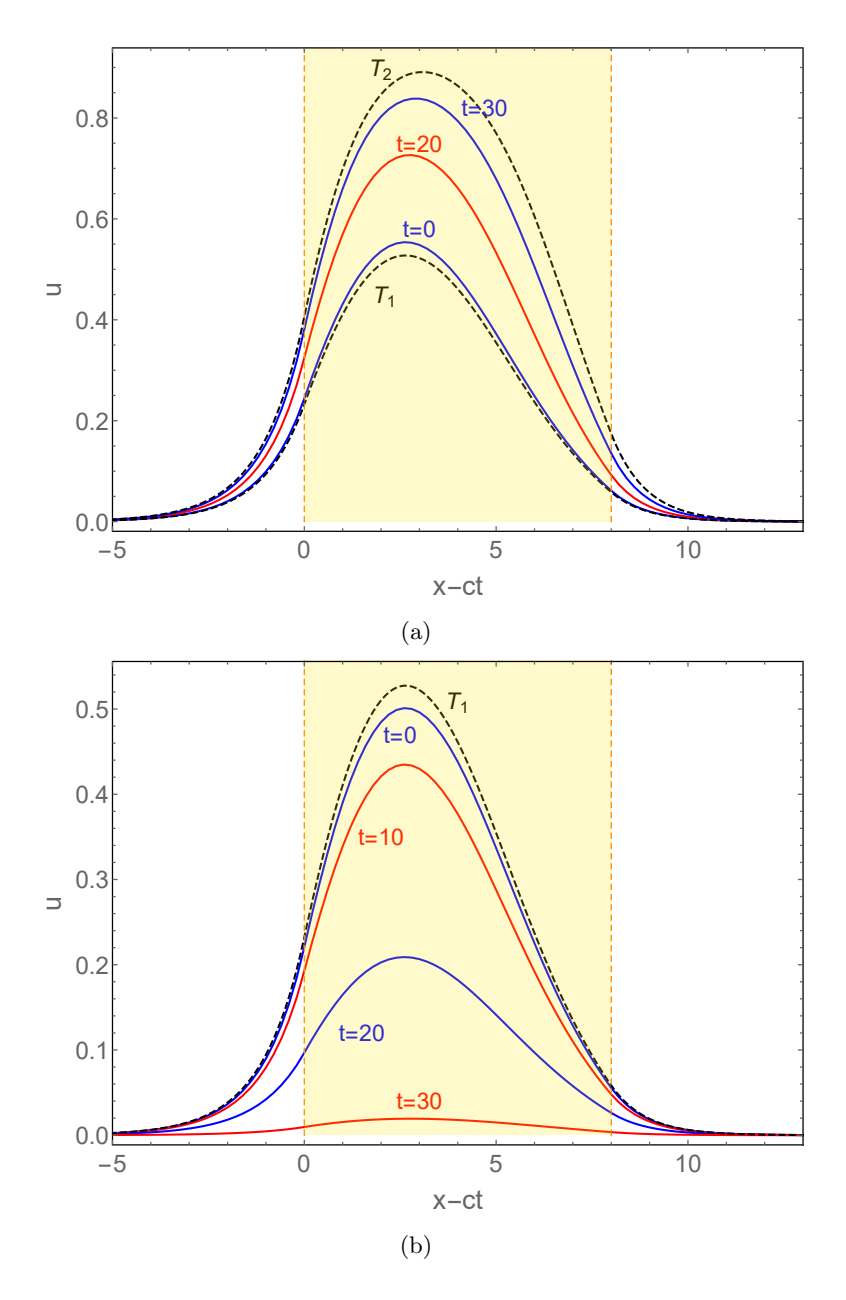


Figure 9: The evolution of solutions initiated near the T_1 equilibrium for parameters $c=0.5c^*$, a=0.2, r=1, and L=8. In (a) we see that a solution initiated 5% above T_1 asymptotically approaches T_2 . In (b) we see that a solutions initiated 5% below T_1 asymptotically approach extinction.

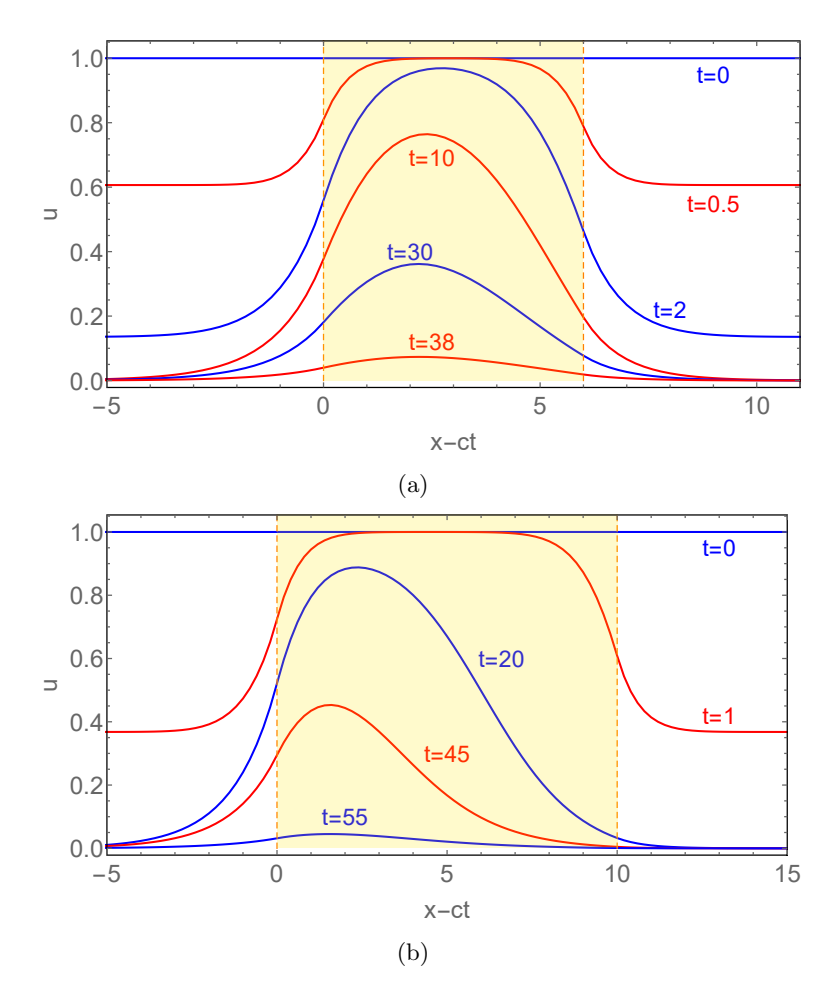


Figure 10: The evolution of a solution leading to extinction. In (a) $L < L^*$. The parameters used are $c = 0.5c^*$, a = 0.2 and r = 1 for which $L^* = 6.79$ but L = 6. In (b) $c = 1.2c^*$ indicating extinction will occur even for a large L. The parameters used are a = 0.2, r = 1 and L = 10.

356 4 Concluding remarks

In this paper, we studied traveling waves for (1.1) and (1.2) with a strong Allee effect in a finite shifting patch of hospitable habitat. We demonstrated that the existence of positive traveling waves is determined by the patch shift speed c, the patch size L, as well as the traveling wave speed c^* of the corresponding system with the same growth function in $(-\infty, \infty)$. Specifically we showed that for $c^* > c > 0$, there exists $L^*(c) > 0$ such that if $L > L^*(c)$ there are two different positive traveling waves with speed c and if $L < L^*(c)$ such a traveling wave does not exist, and for $c > c^*$ there is no positive traveling wave with speed c for any c of these results are supported by our numerical simulations.

Our analysis indicates that positive traveling waves constitute a single-hump profile that vanishes far from origin, and they represent traveling pulses. Such traveling pulses are driven by the shifting patch inside which population grows and outside which population declines. It is well-known that for the reaction-diffusion equation with the reaction term u(a-u)(1-u) (i.e., the Nagumo equation) in a stationary patch with homogeneous Dirichlet boundary conditions, there exist exactly two positive

steady states through a fold bifurcation with the bigger steady state stable and smaller one unstable; see Figure 17.8 in Kot [22]. We conjecture that for $c^* > c$, $L^*(c)$ is the fold bifurcation value, there is exactly one positive traveling wave if $L = L^*(c)$, and there are exactly two positive traveling waves if $L > L^*(c)$ with the bigger (smaller) traveling wave stable (unstable) in (1.1) with (1.2) under Hypotheses 2.1. This conjecture is supported by our numerical simulations which show solutions initiated near but below the lower equilibrium go extinct while those initiated slightly above the lower equilibrium converge to the upper equilibrium (see Fig. 8 and Fig. 9).

It was shown in Berestycki et al. [7] that for (1.1) with no Allee effect, the unique travelig wave (traveling pulse) is globally attracting. As shown in the present paper, the presence of a strong Allee effect leads to the multiplicity of traveling waves (Theorem 2.1(iii)). Our simulations show that the critical patch size $L^*(c)$ increases as c increases (see Fig. 7). This implies that a species persisting in a stationary habitat may eventually die out when the habitat shifts.

The methodology developed in this paper might work for reaction-diffusion models in a shifting patch with other growth functions and boundary conditions. Inside the patch the growth function q(u) could exhibit a weak Allee effect, with an example given by $q(u) = u^2(1-u)$. MacDonald and Lutscher [31] considered a model in a form similar to (1.1) and (1.2) with no Allee effect, different matching boundary conditions and more general movement behavior. The matching conditions in [31] are determined by the probability with which an individual at a boundary point decides to move into or out of the suitable habitat. One may consider a model with a strong Allee effect and the matching conditions given in [31]. The phase plane analysis presented in this paper might be extended to study the existence of positive traveling waves for these models. This paper considered the case of a bounded shifting habitat. It would be of interest to investigate persistence and spread in a reaction-diffusion model with an unbounded shifting habitat and strong Allee effect. The most cited and obvious cause of the Allee effect is the difficulty of finding mates at low population sizes in sexually reproducing species (Boukal and Berec [10], Courchamp et al. [12]). There are works on traveling wave solutions, spreading phenomena, and critical patch sizes for two-sex populations (Ashih and Wilson [3], Maciel et al [32], Miller et al. [33]). It is worth of studying two-sex species models with shifting habitats by extending the framework developed in this paper.

$_{97}$ References

370

371

372

373

374

375

376

377

378

379

380

381

382

383

384

385

386

387

388

389

390

391

392

393

394

395

396

- ³⁹⁸ [1] Aitken SN, Yeaman S, Holliday JA, Wang T, Curtis-McLane S (2008) Adaptation, migration or extirpation: climate change outcomes for tree populations. Evolutionary Applications 1: 95-111.
- [2] Allee WC, Emerson AE, Park O, Park T, Schmidt KP (1949) Principles of animal ecology, W. B Saunders, Philadelphia.
- [3] Ashih AC, Wilson WG (2001) Two-sex population dynamics in space: effects of gestation time on persistence. Theor. Popul. Biol. 60: 93-106.
- [4] Benguria RD, Depassier MC (1996) Speed of fronts of the reaction-diffusion equation. Phys. Rev. Lett. 77: 1171-1173.
- ⁴⁰⁶ [5] Berestycki H, Ross L (2008) Reaction diffusion equations for population dynamics with forced speed. I. The case of the whole space. Discrete Contin. Dyn. Syst. 21: 41-67.

- [6] Berestycki H, Ross L (2009) Reaction diffusion equations for population dynamics with forced speed. II. Cylindrical type domains. Discrete Contin. Dyn. Syst. 25: 19-61.
- [7] Berestycki H, Diekmann O, Nagelkerke CJ, Zegeling PA (2009) Can a species keep pace with a shifting climate? Bull. Math. Biol. 71: 399-429.
- [8] Berestycki H, Fang J (2018) Forced waves of the Fisher-KPP equation in a shifting environment.

 J. Diff. Equ. 264: 2157-2183.
- ⁴¹⁴ [9] Bouhours J, T. Giletti T (2018) Spreading and vanishing for a monostable reaction diffusion equation with forced speed. J. Dyn. Diff. Equ. 31: 247-286.
- ⁴¹⁶ [10] Boukal DS, Berec L (2020) Single-species models of the Allee effect: extinction boundaries, sex ratios and mate encounters. J. Theor. Biol. 218: 375-394.
- Leland EE, Allen JM, Crimmins TM, Dunne JA, Pau S, Travers, SE, Zavaleta ES, Wolkovich EM (2012) Phenological tracking enables positive species responses to climate change. Ecology 93: 1765-1771.
- [12] Courchamp F, Berec L, Gascoigne J (2008) Allee Effects in Ecology and Conservation. Oxford University Press, New York.
- [13] Hu C, Shang J, Li B (2020) Spreading speeds for reaction-diffusion equations with a shifting habitat. J. Dyn. Diff. Equ. 32: 1941-1964.
- ⁴²⁵ [14] J. K. Hale JK (1980) Ordinary Differential Equations, Krieger, Malabar, Florida.
- ⁴²⁶ [15] Du K, Peng R, Sun N (2019) The role of protection zone on species spreading governed by a reaction diffusion model with strong Allee effect. J. Diff. Equ. 266: 7327-7356.
- [16] Fang J, Lou Y, Wu J (2016) Can pathogen spread keep pace with its host invasion? SIAM J. Appl. Math. 76: 1633-1657.
- 430 [17] P.C. Fife, Mathematical Aspects of Reacting and Diffusing Systems, Springer-Verlag, 1979.
- [18] Hadeler KP, Rothe F (1975) Travelling fronts in nonlinear diffusion equations. J. Math. Biol. 2: 251-263.
- [19] Hamel F (1997) Reaction-diffusion problems in cylinders with no invariance by translation. II.

 Monotone perturbations. Ann. Inst. H. Poincaré Anal. Non Linéaire 14: 555-596.
- ⁴³⁵ [20] Hamel F, Roques L (2011) Uniqueness and stability properties of monostable pulsating fronts. J. Eur. Math. Soc. 13: 345-390.
- [21] Kanel' (1962) On the stabilization of solutions of the Cauchy problem for the equations arising in the theory of combustion. Mat. Sbornik 59: 245-288.
- 439 [22] Kot M (2001) Elements of Mathematical Ecology. Cambridge University Press.
- [23] Li B (2012) Traveling wave solutions in partially degenerate cooperative reaction-diffusion systems.
 J. Diff. Equ. 252: 4842-4861.

- Li B, Bewick S, Shang J, Fagan WF (2014) Persistence and spread of a species with a shifting habitat edge SIAM J. Appl. Math. 74: 1397-1417. Erratum to: Persistence and spread of a species with a shifting habitat edge. SIAM J. Appl. Math. 75 (2015) 2379-2380.
- ⁴⁴⁵ [25] Li B, Bewick S, Michael BR, Fagan WF (2016) Persistence and spreading speeds of integrodifference equations with an expanding or contracting habitat. Bull. Math. Biol. 78: 1337-1379.
- ⁴⁴⁷ [26] Li B, Wu J (2020) Traveling waves in integro-difference equations with a shifting habitat. J. Diff. Equ. 268: 40594078.
- ⁴⁴⁹ [27] Li B, Zhang M, Coffman B (2020) Can a barrier zone stop invasion of a population? J. Math. Biol. 81: 1193-1216.
- ⁴⁵¹ [28] Li B, Otto G (2022) Wave speed and critical patch size for integro-difference equations with a strong Allee effect, J. Math. Biol. 85 https://doi.org/10.1007/s00285-022-01814-3.
- ⁴⁵³ [29] Li WT, Wang JB, Zhao XQ (2018) Spatial dynamics of a nonlocal dispersal population model in a shifting environment. J. Nonlinear Science 28: 1189-1219.
- Livshultz T, Mead JV, Goyder DJ, Brannin M (2011) Climate niches of milkweeds with plesiomorphic traits (Secamonoideae; Apocynaceae) and the milkweed sister group link ancient African climates and floral evolution. American Journal of Botany 98: 1966-77.
- ⁴⁵⁸ [31] MacDonald JS, Lutscher F (2018) Individual behavior at habitat edges may help populations persist in moving habitats. J. Math. Biol. 77: 2049-2077.
- 460 [32] Maciel GA, Coutinho RM, Kraenkel RA (2018) Critical patch-size for two-sex populations. Math-461 ematical Biosciences 300: 138-144.
- [33] Miller TEX, Shaw AK, Inouye BD, Neubert MG (2011) Sex-biased dispersal and the speed of two-sex invasions. The American Naturalist 177: 549-561.
- [34] Nagumo J, Yoshizawa S, Arimoto S (1965) Bistable transmission lines. IEEE Trans. Circuit Theory
 CT-12: 400-412.
- Parker IM (2004) Mating patterns and rates of biological invasion. Proc. Natl. Acad. Sci. USA 101: 13695-13696.
- [36] Parmesan C, Yohe G (2003) A globally coherent fingerprint of climate change impacts across natural systems. Nature 421:37-42.
- ⁴⁷⁰ [37] Parmesan C (2006) Ecological and evolutionary responses to recent climate change. Annual Review of Ecology, Evolution, and Systematics 37:637-669.
- Pouchol C, Trélat E, Zuazua E (2019) Phase portrait control for 1D monostable bistable reaction-diffusion equations. Nonlinearity 32: 884-909.
- ⁴⁷⁴ [39] Potapov AB, Lewis MA (2004) Climate and competition: the effect of moving range boundaries on habitat invasibility. Bull. Math. Biol. 66: 975-1008.
- Samuel AK, Chandler RB (2021) An experimental test of the Allee effect range limitation hypothesis Journal of Animal Ecology 90: 585-593.

- ⁴⁷⁸ [41] Shanks AL, Walser A, Shanks L (2014) Population structure, northern range limit, and recruitment variation in the intertidal limpet *Lottia scabra*. Mar. Biol. 161: 10731086.
- Valladares F, Matesanz S, Guilhaumon F et al. (2014) The effects of phenotypic plasticity and local adaptation on forecasts of species range shifts under climate change. Ecology Letters 17: 1351-1364.
- Walther G-R, Post E, Convey P, Menzel A, Parmesa C, Beebee TJC, Fromentin J-M, Hoegh-Guldberg O, Bairlein F (2002) Ecological responses to recent climate change. Nature 416: 389-395.
- Wood C, Fitt RNL, Lancaster LT (2019) Evolving social dynamics prime thermal tolerance during a poleward range shift. Biol. J. Linn. Soc. 126: 574-586.
- ⁴⁸⁷ [45] Zhou Y, Kot M (2011) Discrete-time growth-dispersal models with shifting species ranges. Theor. Ecol. 4:13-25.